



Dual-band optoelectronic poaching detection systems

G. N. MARKUSHIN,^{1,4} V. V. KOROTAEV,^{2,*} A. V. KOSHELEV,^{1,5} I. A. SAMOKHINA,^{1,6}
A. S. VASILEV,^{2,7} A. N. TIMOFEEV,^{2,8} A. V. VASILEVA,^{3,9} AND S. N. YARYSHEV^{2,10}

¹Ural Optical and Mechanical Plant Production Association, Ekaterinburg, Russia

²ITMO University, St. Petersburg, Russia

³M. S. Korp LLC, St. Petersburg, Russia

⁴e-mail: markushin@el.ru

⁵e-mail: avk89122622678@gmail.com

⁶e-mail: irsamoh@mail.ru

⁷e-mail: a_s_vasilev@itmo.ru

⁸e-mail: timofeev@itmo.ru

⁹e-mail: avasileva@itmo.ru

¹⁰e-mail: sniaryshev@itmo.ru

*Corresponding author: korotaev_v_v@mail.ru

Received 9 June 2022; revised 10 June 2022; accepted 11 July 2022; *Opticheskiĭ Zhurnal* **89**, 36–48 (September 2022)

Subject of study. We present details regarding the development of dual-band optoelectronic scanning systems for surveillance and detection of poachers and poaching equipment and the inclusion of image fusion and geolocation capabilities. **Aim.** We present research on a dual-band optoelectronic system for scanning the surface along a quasicircular trajectory that supports overlapping of frames for efficient fusion of images made from different points of view into a single image used to detect, recognize, and geolocate poaching. **Methods.** We present simulation and experimental study of a prototype system including television and thermal vision channels, a Global Positioning System (GPS) antenna, and inertial navigation system modules mounted on a stabilized common platform. **Main results.** We propose a system design that will support simultaneous scanning of a search area in television and thermal imaging channels along a quasicircular trajectory, with the capability to expand the search area and provide 30% frame overlap for efficient image fusion. Gyroscopic sensors on the stabilized common platform for the system and global navigation system antennas will support the requisite accuracy of the surveillance platform and target geolocation. The change in system viewing angle per unit time that would enable the resulting image to be obtained without missing any lines was determined. The primary components of the error in the coordinates of the surveillance platform when surveilling an object were also determined. The combination of field-of-view scanning and use of geolocation equipment supports the recognition of poachers and poaching equipment and the determination of their coordinates within a global coordinate system. An integrated high-precision GPS receiver (ProPak-V3-424) with an inertial system and data processing technology using Tightly Coupled IMU algorithms (Inertial Explorer) was found to be capable of determining the horizontal coordinates of a surveillance platform to within 12 m at a probability of 95% or better. **Practical significance.** A prototype of the proposed design increased the maximum reliable detection and recognition range for poachers and poaching equipment (cars and trucks) in a forest through the fusion of data obtained in the visible and infrared spectral bands. © 2022 Optica Publishing Group

<https://doi.org/10.1364/JOT.89.000528>

1. INTRODUCTION

Poaching—specifically, unlawful hunting or harvesting of natural resources—is a very serious environmental crime with long-term adverse effects on the environment [1,2]. Illegal harvesting of forest products, which makes up as much as 20% of total forest production [3,4], is the most widespread form of poaching in Russia. The large forested land area of Russia means that airborne optoelectronic equipment must be used for timely

detection of poachers and poaching equipment [5–7]. Interest in using improved optoelectronic equipment for detection and identification of poachers and poaching equipment to prevent crimes of this nature has been rising in recent years, both within Russia and around the world.

Poachers and poaching equipment can be efficiently detected using dual- or multi-band optoelectronic systems with detector arrays [8–10]. Most of these systems have a television camera and infrared imager operating in parallel and provide optical

image stabilization. The UltraForce 350/350HD surveillance system manufactured by FLIR Systems [11] is a typical example. However, such systems are not intended for use in scanning mode, leading to lower efficiency.

Data from various spectral regions can be reliably combined by fusion of the images obtained by scanning the field of view [12,13]. It makes sense in this case to use two channels, one sensitive to visible wavelengths (from 0.38 to 0.78 μm) and one sensitive to infrared wavelengths (from 8 to 12 μm). Prior research indicates that such dual-band observations can be used to detect thermal emissions from poachers and poaching equipment, especially when the poachers and poaching equipment are hidden in the forest at different times of day [14].

The purpose of this paper is to research and develop an airborne dual-band optoelectronic system for scanning a site along a quasicircular trajectory that supports overlapping of frames so that images made from different points of view can be efficiently fused into a single image used to detect, recognize, and geolocate poachers and poaching equipment.

In order to achieve this aim, gyroscopically stabilized optoelectronic search and survey devices must be improved [15] in light of techniques for integrating multispectral remote Earth sensing data obtained from airborne platforms [16–19].

The following model poachers or poaching equipment served as video surveillance targets for the research performed herein: a person or group of people, a light automobile or off-road vehicle, a Gazel' small truck/van, an off-road cargo vehicle, a hunting cabin, clear-cut areas, evidence of logging, or combinations of any of these elements.

2. BLOCK DIAGRAM OF THE DUAL-BAND OPTOELECTRONIC SCANNING SYSTEM

When airborne surveillance is performed with dual-band optoelectronic scanning systems (DBOESs), the site of interest is scanned relative to the intended direction of movement of the surveillance platform, the scan results are tied to Global Positioning System (GPS) coordinates, and the observed scenes are recorded along with the flight parameters and observations required for detection and recognition of objects by the operator and ground-based interpretation of the video recordings.

A design was proposed for a DBOES (Fig. 1) consisting of an optoelectronics module and an inertial navigation system (INS) module mounted on a stabilization platform, a stabilization system, a GPS antenna, a monitoring and control unit, and an onboard computer.

The optoelectronics module is the primary functional module for the DBOES and includes television (TV) and thermal imaging (TI) channels with optical systems that produce images in the visible and infrared regions of the spectrum, respectively.

The DBOES is controlled by a monitoring and control unit which includes a system for processing GPS/INS signals, an image processing module, a video recorder, and a monitoring module. The basic functions of the processing and control unit are as follows: control of data transmission between the optoelectronic module and the image processing module, receipt and processing of commands issued by the onboard

computer, and receipt and issuance of commands from and to the ground-based control facility.

The image processing module provides direct control over the operating modes for the TV and TI channels and provides a location for storage of the DBOES parameters. This module also supports fusion of the TV and TI images, while the video recorder provides video recording of the areas being observed. The temperature within the optoelectronic module is thermostatically stabilized for high-quality operation of the TI channel.

The thermostat controls the temperature in the optoelectronic module in conjunction with the monitoring module, which also monitors the performance of the DBOES secondary power sources.

A stabilization system stabilizes the elevation and azimuth of the combined lines of sight for the TV and TI channels.

The effectiveness of detecting poachers and poaching equipment will be substantially greater if each frame is geolocated, i.e., linked to the coordinates of the DBOES within the World Coordinate System and to the angular coordinates of the system line of sight. This is achieved by using the GPS and INS systems in tandem [20]. Airborne DBOESs with direct geolocation capabilities combine the major advantages of INSs and GPS systems while avoiding their major deficiencies [21,22]. The onboard computer software includes standard INS and GPS software.

Both the INS sensors and the optoelectronic module are mounted on a common stabilized platform and support accurate measurement of the platform geolocation and orientation. The INS has three accelerometers and three gyroscopes (for each of the spatial coordinates), as well as angular velocity sensors. INSs have the disadvantage that navigational errors are cumulative, so a GPS antenna is included for improved navigation accuracy.

3. RELATIONSHIP BETWEEN VARIOUS PARAMETERS OF THE SCANNING PROCESS

Quasicircular scanning of the target region is used to extend the DBOES field of view while maintaining high spatial resolution. A complete image of the target region in rectangular format is obtained via horizontal and vertical (perpendicular to the horizontal) scanning, and the resulting image format is determined by the ratio of the corresponding scan rates [23,24]. A review of existing horizontal scan techniques [25,26] revealed that the optimum approach for the TV channel was to rotate the entire optical path about an axis perpendicular to the optical axis and scan direction. In this scan technique, the angular scan speed is equal to the angular scan speed of the TV optical path, meaning the angular speed is limited by the inertia of the mechanical portion of the device. Even if this restriction is observed, a 360° scan can be performed by completely rotating the TV and TI optical paths, so that the DBOES line of sight moves along a circular trajectory.

Scanning with the TI optical path can also be accomplished by rotating the entire optical path about an axis perpendicular to the line of sight. In this approach, the scanning system is smaller than most single-channel designs [22,27] and also faster than the classic two-channel design [23]. The TI channel uses a

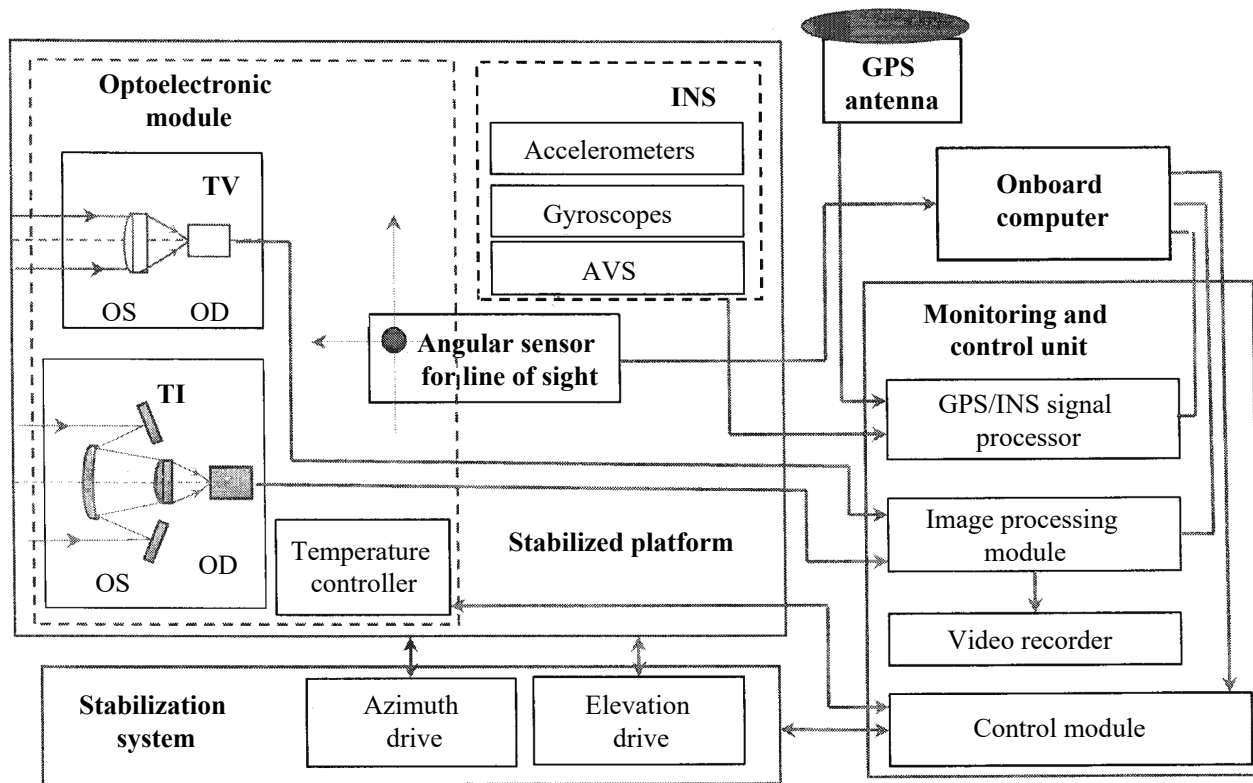


Fig. 1. Block diagram of a direct geolocation DBOES. TV and TI—television and thermal imaging channels, INS—inertial navigation system, AVS—angular velocity sensor, OS—optical system, OD—optical detector.

microbolometer array that is sensitive to wavelengths between 8 and 12 μm [28].

Based on the above discussion, horizontal sweep during scanning of sites is provided by rotating the TV and TI optical paths, which are mounted on a single platform and oriented perpendicular to the line of sight. This approach reduces the size and weight of the DBOES and simplifies synchronization and alignment of the optical paths. Another advantage of this approach is that it provides a much simpler way to produce the vertical scan when performing surveillance from a moving platform since the movement of the DBOES mounted on the platform provides the required scanning trajectory parallel to the platform trajectory (Fig. 2).

In order to prevent lines in the image, the horizontal scan speed must be appropriate for the instantaneous angular dimensions and orientation of the site observed by the DBOES, the platform speed V , and the platform height h ; this requires the derivation of equations for the required rate of change in viewing angle.

The site to be observed is scanned along an arc by varying the azimuth α . The axis of the scanning system is controlled via the elevation angle φ , which is a function of azimuth, meaning that we need to determine the function $\varphi(t)$ to ensure the image remains free of lines.

In a frame-based system model, the coordinates (x_{fr}, y_{fr}) of a point in the optical-system frame are related to the planar coordinates (x, y) of that point in the photogrammetric coordinate system $OXYZ$. During flight, the change in elevation angle φ for the central point in the image while scanning is in progress can

be written in terms of constant speed, flight altitude, and drift angle κ_{dr} . The coordinates $x(t)$ and $y(t)$ of the point where the DBOES line of sight intersects the plane of the horizon at time t are calculated using the following equations [29]:

$$\begin{aligned} x(t) &= V(t - t_0) \cos(\kappa + \kappa_{dr}) - hc_{13}(t)/c_{33}(t), \\ y(t) &= -V(t - t_0) \sin(\kappa + \kappa_{dr}) - hc_{23}(t)/c_{33}(t), \end{aligned} \quad (1)$$

where t_0 is the time at which the scan starts, and $c_{13}(t)$, $c_{23}(t)$, and $c_{33}(t)$ are the components of the direction cosine matrix C [30], which takes into account both the current orientation of the aircraft, described by the matrix C_f (based on the yaw κ , pitch η , and roll ϕ , respectively), and the matrix C_s , determined by the zero angles for the scanning system (the angles κ_0 , η_0 , and ϕ_0). In this case,

$$C = C_s \cdot C_f. \quad (2)$$

The elements $c_{13}(t)$, $c_{23}(t)$, and $c_{33}(t)$ of matrix C are given by

$$\begin{aligned} c_{13}(t) &= c_{f11}(t)c_{s13} + c_{f12}(t)c_{s23} + c_{f13}(t)c_{s33}, \\ c_{23}(t) &= c_{f21}(t)c_{s13} + c_{f22}(t)c_{s23} + c_{f23}(t)c_{s33}, \\ c_{33}(t) &= c_{f31}(t)c_{s13} + c_{f32}(t)c_{s23} + c_{f33}(t)c_{s33}. \end{aligned} \quad (3)$$

The settings matrix takes the form

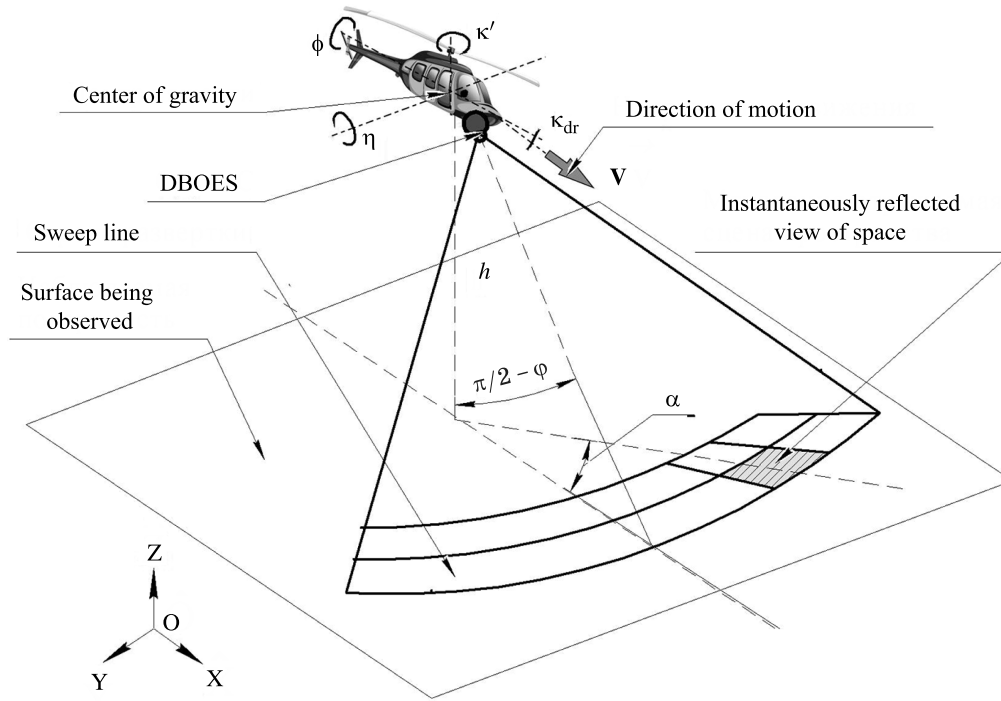


Fig. 2. Diagram of quasicircular scanning. See text for explanation of symbols.

$$C_s = \begin{bmatrix} -\cos \alpha \sin \varphi - \sin \alpha - \cos \alpha \cos(\varphi \phi_0) & \sin(\alpha \phi_0) - \cos \alpha \cos \varphi \\ -\sin \alpha \sin \varphi & \cos \alpha - \sin \alpha \cos(\alpha \phi_0) & -\sin \alpha \cos \varphi - \cos(\alpha \phi_0) \\ \cos \varphi & -\sin \varphi \sin \phi_0 & -\sin \varphi \end{bmatrix}. \quad (4)$$

If the angle ϕ_0 is not known, the following simplified expression for matrix C_s can be used:

$$C_s = \begin{bmatrix} -\cos \alpha \sin \varphi - \sin \alpha - \cos \alpha \cos \varphi \\ -\sin \alpha \sin \varphi & \cos \alpha & -\sin \alpha \cos \varphi \\ \cos \varphi & 0 & -\sin \varphi \end{bmatrix}. \quad (5)$$

Note that using Eq. (5) instead of Eq. (4) will cause uncertainty and reduce the accuracy with which the location of the target could be determined.

The matrix C_f describing the angular position of the platform takes the form

$$C_f = \begin{bmatrix} \cos \kappa \cos \eta & \sin \kappa \cos \phi - \cos \kappa \sin \eta \sin \phi & -\sin \kappa \sin \phi - \cos \kappa \sin \eta \cos \phi \\ -\sin \kappa \cos \phi & \cos \kappa \cos \phi + \sin \kappa \sin \eta \sin \phi & \sin \kappa \sin \eta \cos \phi - \cos \kappa \sin \phi \\ \sin \eta & \cos \eta \sin \phi & \cos \eta \cos \phi \end{bmatrix}. \quad (6)$$

Using Eqs. (1)–(6), the variation in the angle φ is given by

$$x^2(t) + y^2(t) - h^2 \cot^2(\varphi_p) = 0, \quad (7)$$

where φ_p is the fixed offset angle for the scan strip.

The resulting function describing the angle φ as a function of time is quite difficult to write in explicit form. If the pitch of the aircraft is assumed to be equal to zero while scanning is in progress, the yaw will have no effect on the function $\varphi(t)$, and drift is taken into account using α_0 , Eq. (1) will take the form

$$\begin{aligned} x(t) &= V(t - t_0) - h \cos \alpha(t) \cot \varphi(t), \\ y(t) &= -h \sin \alpha(t) \cot \varphi(t), \end{aligned} \quad (8)$$

where t_0 is the time at which $\varphi(t_0) = \varphi_p$ and $\alpha(t_0) = 0$, and the time t is measured relative to the start of the scan.

Substituting Eq. (8) into Eq. (7) leads to the following solution:

$$\varphi(t) = \arctan \left[\frac{\left\{ z + \sqrt{\cot^2 \varphi_p + z^2 \sin^2 \alpha(t)} \right\}}{\left\{ z^2 - \cot^2 \varphi_p \right\}} \right], \quad (9)$$

where $z = (t - t_0)V/h$.

Equation (9) can be used to implement a scanning algorithm, but is fairly complex and may require excessive computational

resources. The equation can be simplified by transformation to a quasicircular survey trajectory, meaning that only the X coordinates are required in Eq. (7) (Fig. 2):

$$\begin{aligned} x(t) &= V(t - t_0) - h \cos \alpha(t) \cot \varphi(t) \\ &= -h \cos \alpha(t) \cot \varphi_p, \end{aligned} \quad (10)$$

which leads to the following final equation for the viewing angle:

$$\varphi(t) = \arctan \left(\cos \alpha(t) / \left[z + \cos \alpha(t) \cot \varphi_p \right] \right). \quad (11)$$

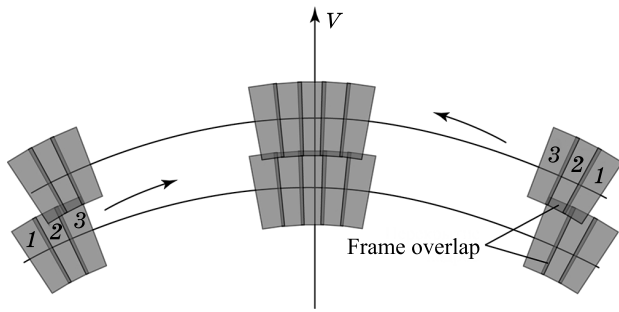


Fig. 3. Image projections for quasicircular scanning of the site.

For any given resolution (determined by the size of the primary target), the angular width of the transverse acquisition band is proportional to the square root of the frame rate divided by the product of the ground speed and flight altitude.

These equations were used for computer modeling to estimate the required longitudinal overlap between strips p [31] in fractions of a frame (Fig. 3) and the required transverse overlap between frames q (in fractions of a frame). The field overlap is determined from the horizontal (transverse overlap) and vertical displacement (longitudinal overlap) of the central point in the image as a function of the flight altitude.

The field overlap during the scan was determined and then graphed (Fig. 4) as a function of α , the rotation angle of the common platform. The graphs indicate that quasicircular scans only provide 30% overlap for angles α between -85° and $+85^\circ$; this should support efficient fusion of images taken at different angles into a single image.

Modeling based on experimental data from flight tests indicated that the average longitudinal overlap between fields should be approximately 30%, with a minimum value of 26%, thereby meeting longitudinal overlap requirements, while transverse overlap should be at least 20% with a mean value of 30%–35%, which is required to ensure the presence of reference points and alignment points for adjacent fields.

4. DIRECT GEOLOCATION ERRORS IN THE DUAL-BAND OPTOELECTRONIC SCANNING SYSTEM

The DBOES geolocation system is unique in that the angular velocity sensors in the DBOES platform stabilization system are fed into the inertial navigation system. The geolocated coordinates of the DBOES are determined by an onboard computer that calculates the position, velocity, and orientation. The GPS system is in turn used to determine the error in the INS and improve the accuracy of the error model. The readings from the INS are continuously compared against the GPS data while the system is in operation [32]. If no satellite signals are available, the software goes into predictive mode, and the current INS data are adjusted in accordance with the precalculated error model. As soon as the GPS reacquires satellites, the software transitions into GPS data smoothing mode and once again starts correcting the INS error model. The combination of GPS satellite data and inertial data provided by the INS means that the GPS eliminates drift and the INS eliminates high-frequency interference so that precise geolocation data can be obtained.

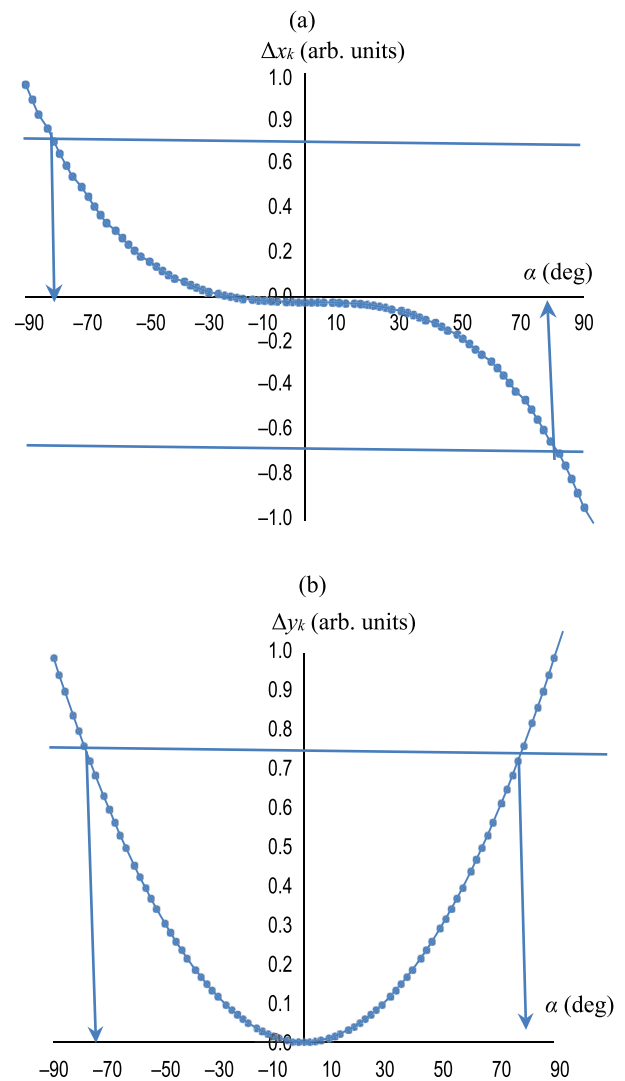


Fig. 4. Graphs of the displacement (a) Δx_k of the central point in the image relative to the length of a frame line (transverse overlap) and (b) Δy_k along a column (longitudinal overlap) as a function of the common platform rotation angle α for a flight altitude of 1 km.

The object coordinates measured by the DBOES include the following major errors:

1. The error of the onboard INS in determining the Cartesian coordinates of the platform, which is of the order of a few dozen meters without the GPS/INS and a few meters with the GPS/INS.
2. The error in the platform yaw, pitch, and roll sensors. For a target range of up to 1 km parallel to the direction of flight and an altitude of 200 m, a pitch measurement error $\Delta\eta = 0.5''$ implies a maximum error of 35 m.
3. Synchronization error between the TV and TI frame rate and the INS measurements, which may amount to a fraction of a second.

For a platform horizontal speed of 100 m/s, a maximum stabilization angle error of $10'$, and a GPS receiver with angular

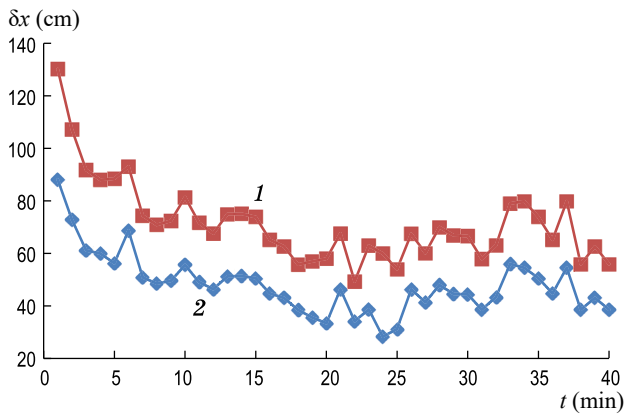


Fig. 5. Estimated error δx in determination of the horizontal coordinates of the helicopter for data processing using the Tightly Coupled IMU algorithm as a function of time t at night (1) and during the day (2).

deviations of 1° amplitude at frequency 1 Hz, a TV and TI channel data synchronization error of 0.1 s will produce a maximum additional horizontal geolocation error of 46 m.

Modeling results using the experimental data obtained showed that a high-precision GPS receiver (ProPak-V3-424) integrated with an INS and use of the NovAtel Tightly Coupled IMU algorithms (Inertial Explorer) [33] for data processing will provide a maximum error δx of 12 m in the horizontal coordinates of the surveillance platform to a probability of 95% or better (Fig. 5).

The constant error component includes an instrumental component caused by residual error in the alignment of the bases of individual DBOES modules.

Using a tightly coupled algorithm to process the original GPS and INS data is an effective solution for high-resolution determination of the DBOES spatial coordinates, velocities, and orientation under conditions where the satellite signals are obstructed.

Processing of the test results determined that the confidence intervals were at the 0.05 level, meaning that the probability of the error in the mean falling within the specified intervals is 0.95. The confidence intervals were found to be quite narrow, i.e., 2 orders of magnitude smaller than the sample mean. This proves that the experiments were accurate and can therefore be considered reliable and trustworthy, as also confirmed by the fact that the maximum dispersion in range was 1 m.

Aligning the centers of the TV and TI observing fields to a maximum error of 12 cm at the target while synchronously monitoring the yaw, pitch, and roll to within a maximum error of 1° will improve the accuracy of coordinates for objects within specified fields of view of the TV and TI channels.

5. EXPERIMENTAL STUDIES OF A PROTOTYPE DUAL-BAND OPTOELECTRONIC SCANNING SYSTEM

The estimated ranges for detection and recognition of object parameters [34] were determined using statistical data obtained during various tests [35].

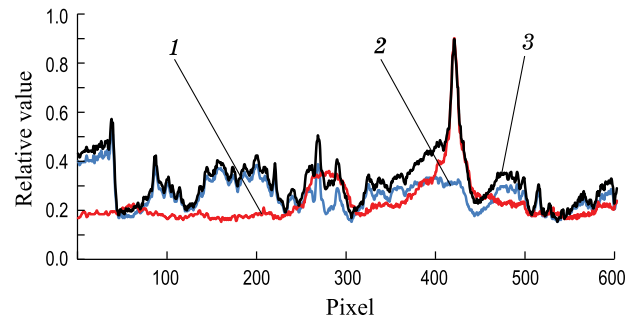


Fig. 6. Graph of the signal distribution in the lines of the digital images from the TV (1) and TI (2) channels and in the fused twilight images (3).

The prototype DBOES underwent a series of full-scale tests to estimate the detection and recognition ranges for targets such as a “person,” a “Gazel” small truck/van,” and a “Ural large truck,” measured on ten flights with a Ka-226 helicopter under day and night conditions. A $1.57 \mu\text{m}$ laser rangefinder with a maximum beam divergence of $2'$ was used to measure the target range to a maximum error of 1 m.

The prototype DBOES experiments were performed at azimuths between -135° and 135° and elevation angles between -110° and 30° . The maximum estimated root-mean-square (RMS) stabilization error for sinusoidal angular variations with amplitude 1° and frequency 1 Hz was $10'$. The maximum estimated RMS error in the angular coordinates describing the position of the system modules relative to their mounts was $3'$, and the maximum angular motion of the line of sight in stabilization mode was 30 deg/s. The relative contrast between object and background varied from 0.1 to 0.5.

The TI channel was used for wavelengths of 8 to $12 \mu\text{m}$, with a 768×576 pixel TI raster format and a minimum threshold temperature differential of 35 mK.

The television channel was used for wavelengths of 0.38 to $12 \mu\text{m}$, with a 1280×960 pixel television raster format and a minimum threshold illuminance of 0.5 lux.

These experiments were performed with the TV and TI channels synchronized, $6^\circ \times 8^\circ$ instantaneous fields of view and a minimum update rate of 50 Hz.

Over the course of ten flights, in which the angular velocities of the targets in the scan strip relative to the helicopter did not exceed 10 deg/s, we found that even though the estimated probability of target recognition by an operator had a confidence level of 0.38, the actual probability of target recognition was at least 0.8.

When fusing images from different spectral bands, the TI channel is frequently used to improve the observational capability for analysis of the thermal field and provides cues to the operator and system in the form of corresponding image markers. Recognition is generally performed using the higher-resolution visible channel.

Testing revealed that the TV channel was most effective under daytime conditions, the TI channel was most effective under nighttime conditions, and the fused image was best under twilight conditions.

Figure 6 shows a graph of the signal distribution in the TV and TI channel lines and in the fused twilight images.

Table 1. Results from Testing a Prototype DBOES for the Detection and Recognition of Poaching-Related Targets

Test Series Number	Channel	Target	Time of Day	Weather Conditions			Flight Mode		Test Results	
				MOR ^a (km)	Air Temperature (°C)	Relative Humidity (%)	Flight Speed (km/h)	Flight Altitude (m)	Detection	Recognition
1	TV	Person	Day	9	25	95, periodic light rain	160	30–150	2000	950
2	TV + TI	Person	Day	9	25	95, periodic light rain	160	30–150	2400	1200
3	TI	Person	Night	10	21	95	170	30–150	2500	1100
4	TV	Gazel' small truck/van	Day	9	25	95, periodic light rain	160	30–150	3000	1500
5	TV + TI	Gazel' small truck/van	Day	9	25	95, periodic light rain	160	30–150	8000	3500
6	TI	Gazel' small truck/van	Night	8	21	95	160	30–150	8300	4000
7	TI	Ural large truck	Day, 15:00–17:30	10	21	40	170	300–500	8500	4400
8	TV + TI	Ural large truck	Day, 15:00–17:30	10	21	40	170	300–500	12000	5700
9	TV	Ural large truck	Evening, 18:00–20:00	10	19	43	180	300–500	8500	4300
10	TV + TI	Ural large truck	Evening, 18:00–20:00	9	19	43	180	300–500	14500	5400
11	TI	Ural large truck	Night, 21:00–23:30	9	14	48	170	300–500	8300	3300
12	TV	Hunting cabin	Day, 15:00–17:30	10	21	44	170	300–500	3600	1350
13	TV + TI	Hunting cabin	Day, 15:00–17:30	10	21	44	170	300–500	4600	2150

^aMOR—meteorological optical range.

The plotted lines in Fig. 6 indicate that individual TV and TI images contain higher-contrast areas while the fused image has higher contrast along the entire line, thereby increasing the information content of the combined signal, leading to a higher probability of target detection.

Table 1 presents DBOES target detection and recognition test results under a variety of conditions. Most of the tests were performed during daylight hours.

Test series 3, 6, and 11 were performed at night, so the TI channel was primary. Higher thermal contrast enabled us to detect objects at longer range; however, the inability to fuse the TV and TI images reduced the maximum recognition range. Preliminary tests indicated that the thermal contrast in the TI channel images is insufficient for reliable target recognition if used alone (Fig. 6).

Test series 7–13 for detection of the “Ural large truck” and “hunting cabin” targets were performed during the daytime, evening, and nighttime. Detection of the “Ural large truck” target was performed with a large field of view for the TV and TI channels. The targets were recognized within a small field of view using the image on the monitor screen.

The tests revealed that for a helicopter speed of 100 m/s; a TV camera field of view $\theta = 3^\circ$ along the short side of the raster for ranges of 3000, 4000, and 5000 m; and angular scan speeds of up to 10 deg/s, target recognition based on the video recording was 2 times worse than using the onboard display.

The tests showed that data fusion provides an advantage during twilight. Switching to TV + TI channel data fusion mode provides higher-quality video images and increases the range at which targets can be detected, thereby significantly enhancing the operational capability of the DBOES.

The DBOES test results were used to develop a line of optical surveillance systems to be manufactured by the Ural Optical and Mechanical Plant Production Association [15] that are appropriate for a wide range of modern search and detection tasks involving a variety of targets at ranges of up to 20 km (motor vehicles, people, fire hot spots, oil and gas leaks, power transmission lines, etc.).

These optical surveillance systems appear to have similar parameters and specifications to those of the closest similar device—the FLIR UltraForce 350 [11]; however, the functional capabilities of the SON-530 are somewhat better.

The SON line has the advantage that it uses open architecture, meaning that the devices can be installed on any platform and a peripheral with that platform can be used by means of a standard data transfer protocol (RS-422, RS-485, RS-232).

6. CONCLUSION

A design was proposed for a dual-band optoelectronic aircraft-based surveillance system with TV and TI channels, INS sensors, and a GPS receiver to provide longer-range detection and recognition of poachers and poaching equipment during

daytime, nighttime, and twilight by means of processing and fusing video information in the visible and infrared bands.

Validation was obtained for the concept of scanning the field along a quasicircular trajectory by rotation of the TV and TI optical paths mounted on a single platform, with the sweep (in the perpendicular direction) being produced via the flight path of the platform, providing the 30% frame overlap required in order not to miss any detectable targets.

The change in system viewing angle per unit time was determined so that the desired overlap could be maintained in the resulting image without missing any lines.

The modeling results confirm that a DBOES having a high-precision GPS receiver (ProPak-V3-424) integrated with an INS and data processing technology using Tightly Coupled IMU algorithms (Inertial Explorer) is capable of determining the horizontal coordinates of a helicopter to within 12 m at a probability of 95% or better.

Full-scale experimental studies using the DBOES in search and detection mode to detect poachers and poaching equipment in a forest indicated that the detection and recognition range was at least 8% longer if image fusion was used, especially for flights during twilight.

REFERENCES

- V. D. Larichev, E. O. Derevyanko, and V. T. Mazein, "Characteristics of corruption-related phenomena in natural resources use and protection," *Advokat* (12), 71–90 (2004).
- I. A. Konforkin, "Political, legal, and economic aspects of forest poaching," in *Sociopolitical Processes in a Changing World*, V. P. Gavrikovaya, ed. (Tverskoy Gosudarstvennoy Universitet, Tver', 2018), pp. 79–82.
- V. I. Sukhikh, "Illegal logging in Russia and approaches for eliminating it," *Lesn. Khoz.* (4), 31–53 (2005).
- É. D. Guseinova and E. V. Maksimova, "Anti-poaching efforts on the Russian–Chinese border," *Aktual. Probl. Nauki Prakt.* (3), 52–55 (2021).
- O. V. Skudneva, "Drones in the Russian forest management system," *Izv. Vyssh. Uchebn. Zaved. Lesn. Khoz.* (6), 150–154 (2014).
- S. V. Koptev and O. V. Skudneva, "Opportunities for drone usage in forest management," *Izv. Vyssh. Uchebn. Zaved. Lesn. Khoz.* (1), 130–138 (2018).
- A. Rango, A. Laliberte, J. E. Herrick, C. Winters, K. Havstad, C. Steele, and D. Browning, "Unmanned aerial vehicle-based remote sensing for rangeland assessment, monitoring, and management," *J. Appl. Remote Sens.* **3**(1), 033542 (2009).
- V. V. Tarasov and Yu. G. Yakushenkov, *Dual-Band and Multi-spectral Optoelectronic Systems with Array Detectors* (Universitetskaya Kniga, Moscow, 2007; Logos, 2007).
- D. Farrah, K. E. Smith, D. Ardila, et al., "Far-infrared instrumentation and technological development for the next decade," *J. Astron. Telesc. Instrum. Syst.* **5**(2), 020901 (2019).
- V. S. Goryainov, A. A. Buznikov, and V. I. Chernook, "Usage of lidar systems for environmental monitoring," *Izv. S.-Peterb. Gos. Élektrotekh. Univ. LÉTI* (9), 22–30 (2012).
- "Aircraft-based surveillance systems," *Diagnostics World*, <https://diaworld.ru/production/111/>.
- N. I. Pavlov and G. I. Yasiniskii, "Compact airborne multispectral scanning device," *J. Opt. Technol.* **77**(3), 207–211 (2010) [Opt. Zh. **77**(3), 67–72 (2010)].
- V. V. Eremeev and A. É. Moskvitin, "Current issues in fusion of images from different remote Earth sensing systems," *Radiotekhnika (Moscow)* **84**(11(21)), 89–100 (2020).
- G. N. Markushin, V. V. Korotaev, A. V. Koshelev, I. A. Samokhina, A. S. Vasil'ev, A. V. Vasil'eva, and S. N. Yaryshev, "Image fusion in a dual-band scanning optoelectronic system for the search and detection of poaching activity," *J. Opt. Technol.* **87**(6), 365–370 (2020) [Opt. Zh. **87**(6), 57–65 (2020)].
- "Ural Optical and Mechanical Plant Production Association Joint-Stock Corporation optical surveillance systems," 2020, <http://www.uomz.ru/production/optical-observation-system>.
- Y. Zhou, L. Wang, K. Jiang, L. Xue, F. An, B. Chen, and T. Yun, "Individual tree crown segmentation based on aerial image using superpixel and topological features," *J. Appl. Remote Sens.* **14**(2), 022210 (2020).
- A. E. Effiom, L. M. van Leeuwen, P. Nyktas, J. A. Okojie, and J. Erdbrügger, "Combining unmanned aerial vehicle and multispectral Pleiades data for tree species identification, a prerequisite for accurate carbon estimation," *J. Appl. Remote Sens.* **13**(3), 034530 (2019).
- A. S. Vasil'ev, A. V. Krasnyashchikh, V. V. Korotaev, O. Yu. Lashmanov, D. Yu. Lysenko, O. N. Nenarokomov, A. S. Shirokov, and S. N. Yaryshev, "Development of a hardware and software system for forest fire detection by image fusion," *Izv. Vyssh. Uchebn. Zaved. Priborostr.* **55**(12), 50–56 (2012).
- A. S. Vasilev and V. V. Korotaev, "Research of the fusion methods of the multispectral optoelectronic systems images," *Proc. SPIE* **9530**, 953007 (2015).
- E. M. Medvedev, I. M. Danilin, and S. R. Mel'nikov, *Laser Ranging of Land and Forests (Geolidar: Geokosmos, Moscow, 2007)*
- A. I. Altukhov and D. S. Korshunov, "Method for identifying changes in the condition of the Earth surface using space-based photographs obtained at different times," *Nauchno-Tekhn. Vestn. Inf. Tekhnol. Mekh. Opt.* **19**(3), 410–416 (2019).
- M. L. Belov, V. A. Gorodnichev, V. Ya. Kolyuchkin, and S. B. Odinkov, *Satellite-Based Optoelectronic Environmental Monitoring Systems* (Izd. MG TU im. N. É. Bauman, Moscow, 2014).
- A. S. Makarov, A. I. Omelaev, and V. L. Filippov, *Introduction to Technology for the Development and Assessment of Scanning Television Systems* (Unipress, Kazan', 1998).
- S. V. Medushev, V. E. Remizov, and V. V. Shichkov, "Promising options for construction of programmable two-coordinate steerable scanning mirrors," *Vopr. Élektromekh. Tr. VNIIEM* **107**, 32–37 (2008).
- M. M. Miroshnikov, *Fundamentals of Optoelectronic Instruments*, 3rd ed. (Lan', St. Petersburg, 2010).
- A. H. Lettington, I. M. Blankson, M. F. Attia, and D. Dunn, "Review of imaging architecture," *Proc. SPIE* **4719**, 327–340 (2002).
- V. V. Korotaev, G. S. Mel'nikov, S. V. Mikheev, V. M. Samkov, and Yu. I. Soldatov, *Fundamentals of Thermal Engineering* (NIU ITMO, St. Petersburg, 2012).
- N. Kul'chitskii, A. Naumov, and V. Startsev, "Current status and trends on the uncooled microbolometer market," *Tekhnol. Zashch.* **2**, 55–57 (2018).
- V. I. Fedorov, *Engineering Aerogeodesy* (Nedra, Moscow, 1988).
- V. P. Kovalenko, *Photogrammetric Processing of Materials from Airborne Reconnaissance Imaging Equipment* (VVIA im. Prof. N. E. Zhukovskogo, Moscow, 2003).
- R. V. Zotov, *Aerogeodesy* (SibADI, Omsk, 2012), Vol. 1.
- G. W. Hein, "From GPS and GLONASS via EGNOS to Galileo—positioning and navigation in the third millennium," *GPS Solutions* **3**(4), 39–47 (2000).
- E. A. Plyusnin, "Advantages from the integration of satellite positioning systems and inertial measurement devices," <http://www.gisa.ru/49205.html>.
- GOST R 8.619-2006, "State system for ensuring uniformity of measurements," 2006.
- G. N. Gryazin, *Applied Television Fundamentals and Systems*, N. K. Mal'tsev, ed. (Politekhnik, St. Petersburg, 2011).

Gregory N. Markushin—E. S. Yalamov Ural Optical and Mechanical Plant Production Association, Ekaterinburg, Russian Federation; Scopus ID 57218767952; <https://orcid.org/0000-0003-1611-7353>; markushin@e1.ru

Valery V. Korotaev—Doctor of engineering sciences, Professor, ITMO University, St. Petersburg, 197101, Russia; Scopus ID 6603855670; <https://orcid.org/0000-0001-7102-5967>; korotaev_v_v@mail.ru

Alexander V. Koshelev—E. S. Yalamov Ural Optical and Mechanical Plant Production Association, Yekaterinburg, Russian Federation; Scopus ID 57218771679; <https://orcid.org/0000-0002-1126-4031>; avk89122622678@gmail.com

Irina A. Samokhina—Candidate of engineering sciences, Ural Optical and Mechanical Plant Production Association, St. Petersburg, Russian Federation; <https://orcid.org/0000-0002-4818-2785>; irsamoh@mail.ru

Aleksandr S. Vasilev—Candidate of engineering sciences, Associate Professor, ITMO University, St. Petersburg, 197101, Russia; Scopus ID 24468859400; <https://orcid.org/0000-0002-2080-3252>; a_s_vasilev@itmo.ru

Alexander N. Timofeev—Candidate of engineering sciences, Senior Researcher, Lead Engineer, ITMO University, St. Petersburg, 197101, Russia; Scopus ID 57189271286; <https://orcid.org/0000-0002-7344-9832>; timofeev@itmo.ru

Anna V. Vasileva—Candidate of engineering sciences, Algorithm Developer, M. S. Korp, St. Petersburg, 195009, Russia; Scopus ID 56556815200; <https://orcid.org/0000-0002-6020-7017>; avasileva@itmo.ru

Sergey N. Yaryshev—Candidate of engineering sciences, Associate Professor, ITMO University, St. Petersburg, 197101, Russia; Scopus ID 56027828300, 36338225400; <https://orcid.org/0000-0001-9421-8446>; sniaryshev@itmo.ru